White Rose Research Online

eprints@whiterose.ac.uk
https://eprints.whiterose.ac.uk
Universities of Leeds, Sheffield and York

Deposited via The University of York.

White Rose Research Online URL for this paper:
https://eprints.whiterose.ac.uk/id/eprint/202255/

Version: Published Version

**Article:**
Kuntová, Lucie, Mašlanová, Ivana, Oborilová, Radka et al. (2023) Staphylococcus aureus Prophage-Encoded Protein Causes Abortive Infection and Provides Population Immunity against Kayviruses. MBio. e02490-22. ISSN: 2150-7511

https://doi.org/10.1128/mbio.02490-22

**Reuse**
This article is distributed under the terms of the Creative Commons Attribution (CC BY) licence. This licence allows you to distribute, remix, tweak, and build upon the work, even commercially, as long as you credit the authors for the original work. More information and the full terms of the licence here: https://creativecommons.org/licenses/

**Takedown**
If you consider content in White Rose Research Online to be in breach of UK law, please notify us by emailing eprints@whiterose.ac.uk including the URL of the record and the reason for the withdrawal request.

UNIVERSITY OF LEEDS
University of Sheffield
UNIVERSITY of York

AMERICAN SOCIETY FOR MICROBIOLOGY | mBio®

RESEARCH ARTICLE

# *Staphylococcus aureus* Prophage-Encoded Protein Causes Abortive Infection and Provides Population Immunity against Kayviruses

**Lucie Kuntová,[a] Ivana Mašlaňová,[a] Radka Obořilová,[a,b,c] Hana Šimečková,[a] Adéla Finstrlová,[a] Pavol Bárdy,[d] Marta Šiborová,[b] Liudmyla Troianovska,[a] Tibor Botka,[a] Petr Gintar,[b,e] Ondrej Šedo,[b] Zdeněk Farka,[a,b,c] Jiří Doškař,[a] Roman Pantůček[a]**

[a]Department of Experimental Biology, Faculty of Science, Masaryk University, Brno, Czech Republic
[b]Central European Institute of Technology, Masaryk University, Brno, Czech Republic
[c]Department of Biochemistry, Faculty of Science, Masaryk University, Brno, Czech Republic
[d]Department of Chemistry, York Structural Biology Laboratory, University of York, York, United Kingdom
[e]National Centre for Biomolecular Research, Faculty of Science, Masaryk University, Brno, Czech Republic

Lucie Kuntová and Ivana Mašlaňová contributed equally to this work. Author order was determined alphabetically.

**ABSTRACT** Both temperate and obligately lytic phages have crucial roles in the biology of staphylococci. While superinfection exclusion among closely related temperate phages is a well-characterized phenomenon, the interactions between temperate and lytic phages in staphylococci are not understood. Here, we present a resistance mechanism toward lytic phages of the genus *Kayvirus*, mediated by the membrane-anchored protein designated $Pdp_{Sau}$ encoded by *Staphylococcus aureus* prophages, mostly of the Sa2 integrase type. The prophage accessory gene $pdp_{Sau}$ is strongly linked to the lytic genes for holin and ami2-type amidase and typically replaces genes for the toxin Panton-Valentine leukocidin (PVL). The predicted $Pdp_{Sau}$ protein structure shows the presence of a membrane-binding $\alpha$-helix in its N-terminal part and a cytoplasmic positively charged C terminus. We demonstrated that the mechanism of action of $Pdp_{Sau}$ does not prevent the infecting kayvirus from adsorbing onto the host cell and delivering its genome into the cell, but phage DNA replication is halted. Changes in the cell membrane polarity and permeability were observed from 10 min after the infection, which led to prophage-activated cell death. Furthermore, we describe a mechanism of overcoming this resistance in a host-range *Kayvirus* mutant, which was selected on an *S. aureus* strain harboring prophage 53 encoding $Pdp_{Sau}$, and in which a chimeric gene product emerged via adaptive laboratory evolution. This first case of staphylococcal interfamily phage-phage competition is analogous to some other abortive infection defense systems and to systems based on membrane-destructive proteins.

**IMPORTANCE** Prophages play an important role in virulence, pathogenesis, and host preference, as well as in horizontal gene transfer in staphylococci. In contrast, broad-host-range lytic staphylococcal kayviruses lyse most *S. aureus* strains, and scientists worldwide have come to believe that the use of such phages will be successful for treating and preventing bacterial diseases. The effectiveness of phage therapy is complicated by bacterial resistance, whose mechanisms related to therapeutic staphylococcal phages are not understood in detail. In this work, we describe a resistance mechanism targeting kayviruses that is encoded by a prophage. We conclude that the defense mechanism belongs to a broader group of abortive infections, which is characterized by suicidal behavior of infected cells that are unable to produce phage progeny, thus ensuring the survival of the host population. Since the majority of staphylococcal strains are lysogenic, our findings are relevant for the advancement of phage therapy.

**Editor** Alison Buchan, University of Tennessee at Knoxville

**Copyright** © 2023 Kuntová et al. This is an open-access article distributed under the terms of the Creative Commons Attribution 4.0 International license.

Address correspondence to Roman Pantůček, pantucek@sci.muni.cz.

The authors declare no conflict of interest.

**Received** 19 September 2022
**Accepted** 19 January 2023
**Published** 13 February 2023

Downloaded from https://journals.asm.org/journal/mbio on 08 August 2023 by 144.32.224.27.

**KEYWORDS** *Staphylococcus aureus*, lysogeny, phage resistance, abortive infection, *Kayvirus*, cell death, phage therapy, bacteriophage evolution, bacteriophage therapy, bacteriophages

Bacteriophages are widespread across ecosystems and are among the most numerous entities on earth. Bacteria are constantly threatened by phage infection, and 20 to 40% of daily bacterial death is caused by bacteriophages (1). Conversely, the integrated genomes of prophages often promote beneficial phenotypic changes in their hosts (2) and play a major role in horizontal gene transfer, thus contributing to the evolution of bacterial pathogens (3).

Most *Staphylococcus aureus* isolates carry multiple siphoviral prophages in their genome (4) with an impact on virulence, toxin production, immune evasion, and host preference (5) as well as the mobilization of variable genetic elements (6) and dissemination of antibiotic resistance by transduction (7–9). Besides temperate staphylococcal siphoviruses, there are the strictly lytic myoviruses (10) and podoviruses (11) that are believed to be suitable for use as antimicrobial agents.

Over the last 2 decades, interest in using phages for the treatment of bacterial infections has increased enormously. Based on current clinical trials, phage therapy is efficient, safe, and acceptable for treatment in human medicine (12). The therapeutic potential of kayviruses with the type phage K (13) led to the characterization of many phage strains of this genus with an extremely broad host range (14) as was demonstrated for phage 812 (15). Kayviruses were studied to clarify their polyvalence (15, 16), lytic activity (17–19), synergistic effect with antibiotics (20), and interaction with the immune system (21); to describe their structure and genome delivery (22); and for safety assessments for therapy (23, 24). This progress in the implementation of kayviruses into safe phage therapy has been achieved by the characterization of staphylococcal phage-host interactions at the omics level, such as comparative genomics (10, 14, 15, 25), transcriptomics (26, 27), and proteomics studies (28).

One of the limitations of using kayviruses in medical practice is the possible resistance of staphylococcal species to these phages. During the constant competition between phages and their hosts, multiple bacterial phage resistance systems targeting various stages of the phage life cycle have evolved (29, 30). In staphylococci, these include various mechanisms, such as targeting foreign DNA by restriction modification (31), CRISPR-Cas immunity (32), protection against entry into the host cell through the modification of wall teichoic acids (33), overproduction of staphylococcal protein A (34), prophage-induced immunity (35), interference with phage reproduction mediated by pathogenicity islands (36), and the different host factors required for phage reproduction (37).

Some antiphage systems in staphylococci are yet to be discovered, namely, the large group of mechanisms categorized as abortive infections. Here, we report that temperate siphoviruses can protect the staphylococcal population from destruction by virulent *Kayvirus* phages by an abortive infection mechanism.

## RESULTS AND DISCUSSION

**Prophages induce insensitivity of *S. aureus* to kayviruses.** Prophageless *S. aureus* strains ISP8 and 1039 were lysogenized by prophages 11, 29, 42E, 47, 53, 71, 77, 80$\alpha$, 83A, 84, 85, or 96 and tested for susceptibility to lytic kayviruses 812, 812a, and K. The integration of prophages 47, 53, and 80$\alpha$ resulted in a resistant phenotype to the lytic phages 812 and K. Phage 53 was used for the lysogenization of multiple strains, including methicillin-resistant *S. aureus* (MRSA) USA300 (Table 1), which led to the establishment of a resistant phenotype to phages 812 and K independently of the genetic background of the lysogens. In models of cured strains NCTC 8511 (53$^+$)c and ISP8 (53$^+$)c, it was shown that sensitivity to both phages 812 and K is renewed after the prophage is lost. Similarly, *S. aureus* NCTC 8325, which is naturally resistant to phage 812, regained its sensitivity after all of its prophages were removed (Table 1). In contrast to phages 812 and K, prophages 47, 53, and 80$\alpha$ do not affect sensitivity to phage 812a, the phage 812 host-range mutant that originated during passaging phage 812 on *S. aureus* strain NCTC 8511 with prophage 53 (38) (Table 1).



Downloaded from https://journals.asm.org/journal/mbio on 08 August 2023 by 144.32.224.27.

**TABLE 1** Staphylococcal strains used in this study and their sensitivity to lytic phages[a]

| Bacteria and strain | Presence of $pdp_{Sau}$ | Prophage content; strain characteristics | Reference or source | Sensitivity to kayvirus | | |
|---|---|---|---|---|---|---|
| | | | | K | 812 | 812a |
| *S. aureus* | | | | | | |
| RN4220 | − | No prophage; propagation strain for phage K | 95 | + | + | + |
| CCM 4028 (= SA812) | − | Sa2int, Sa3int; propagation strain for phage 812 | 38 | + | + | + |
| RN4220 (pCN51) | − | No prophage | This study | + | + | + |
| RN4220 (pCN51-$pdp_{Sau}$) | + | No prophage | This study | − | − | + |
| RN4220 (pCN51-$pdp_{Sau}$-orf812a_191) | + | No prophage | This study | + | + | + |
| RN4220 ($53^+$) | + | Sa7int | This study | − | − | + |
| RN4220 ($53^+$) (pCN51-orf812a_191) | + | Sa7int | This study | + | + | + |
| NCTC 8325 | + | Sa2int, Sa3int, Sa5int | Culture collection | − | − | + |
| ISP8 (= 8325-4) | − | No prophage; cured for phi11, phi12, phi13 | 96 | + | + | + |
| ISP8 ($47^+$) | + | Sa2int | This study | − | − | + |
| ISP8 ($53^+$) | + | Sa7int | 64 | − | − | + |
| ISP8 ($53^+$)c | − | No prophage; cured for phi53 | 64 | + | + | + |
| 1039 (= CCM 4890) | − | No prophage | 97 | + | + | + |
| NCTC 8511 | − | Sa2int, Sa3int, Sa6int | Culture collection | + | + | + |
| NCTC 8511 ($53^+$) (= S26) | + | Sa2int, Sa3int, Sa6int, Sa7int | 38 | − | − | + |
| NCTC 8511 ($53^+$)c | − | Sa2int, Sa3int, Sa6int, cured for phi53 | This study | + | + | + |
| USA300 | − | Sa2int, Sa3int | 98 | + | + | + |
| USA300c | − | No prophage; cured for $phiSa2_{USA}$ and $Sa3_{USA}$ | 99 | + | + | + |
| USA300c ($53^+$) | + | Sa7int | This study | − | − | + |
| E48 (= NRL 02/947) | + | Sa2int, Sa3int, clinical MRSA isolate | 100 | − | − | + |
| *S. epidermidis* | | | | | | |
| Tü 3298 | − | ND | 101 | + | + | − |
| Tü 3298 (pCN51-$pdp_{Sau}$) | + | ND | This study | − | − | − |

[a]+, sensitive; −, resistant; ND, not determined.

The studied prophages 47, 53, and 80$\alpha$ that induced immunity to kayviruses 812 and K are unrelated or only distantly related to each other based on their whole-genome sequence. Phage 47 belongs to group A by the original serological classification and to integrase type Sa2. Phages 53 and 80$\alpha$ belong to group B and integrase types Sa7 and Sa5, respectively. Each integrase type possesses a different *att* site; thus, the insertion inactivation of a bacterial gene is not the cause of the induced nonsensitivity. Comparative genomic analyses of phages 47, 53, and 80$\alpha$ revealed only one common gene corresponding to ORF016 coding for an unknown protein (UniProtKB accession no. Q4ZDJ8) in the previously published bacteriophage 53 genome (39). This gene was designated $pdp_{Sau}$ (phage defense protein of *S. aureus*).

A set of MRSA strains was subsequently screened for the $pdp_{Sau}$ gene using PCR. All $pdp_{Sau}$-positive strains exhibited resistance to wild-type phage 812. Strain E48 (ST8/t024/staphylococcal cassette chromosome *mec* element IV [SCC*mec* IV]) related to USA300 (40) as a representative of the most frequent genotype that naturally carried the $pdp_{Sau}$ gene (Table 1) was genome sequenced and used for further analyses.

**Phage sensitivity assay in an artificial expression system.** To verify the direct association between the $pdp_{Sau}$ gene and a phage-resistant phenotype, the $pdp_{Sau}$ gene was cloned in the expression vector pCN51 under a cadmium-inducible promoter (41) and electroporated into *S. aureus* RN4220, which is naturally sensitive to phages 812 and K. The $Pdp_{Sau}$ protein was detected by mass spectrometry after SDS-PAGE of the proteins from lysed cells both in the naturally occurring lysogen and the artificial system, where 28% of the protein sequence (amino acid range 39 to 178) was covered by nine tryptic peptides. A strain harboring the construct pCN51-$pdp_{Sau}$ exhibited a resistant phenotype to both phages after the overexpression, the same as the lysogenic strain *S. aureus* RN4220 ($53^+$) (Fig. 1A). This proved that the protein $Pdp_{Sau}$ alone is sufficient to induce resistance to phages 812 and K. Next, the construct pCN51-$pdp_{Sau}$ was transformed into the coagulase-negative *Staphylococcus epidermidis* Tü 3298 strain (Table 1), where the expression of the $pdp_{Sau}$ gene also led to the induction of a resistant phenotype.



Downloaded from https://journals.asm.org/journal/mbio on 08 August 2023 by 144.32.224.27.

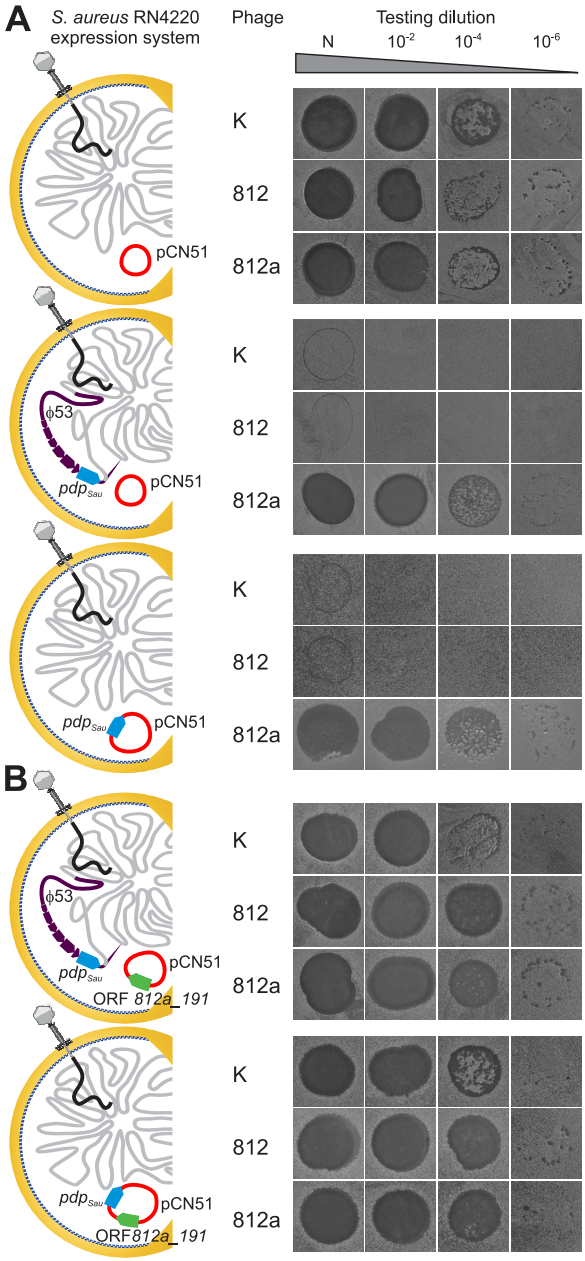


**FIG 1** Impact of $pdp_{Sau}$ gene expression on *Kayvirus* lytic action demonstrated by drop assay performed with phages K, 812, and 812a on *S. aureus* RN4220 derivatives. Testing was performed at four phage concentrations, nondiluted phage with a titer of $10^9$ PFU/mL (N) and dilutions of $10^{-2}$, $10^{-4}$, and $10^{-6}$. Four types of resulting lytic zones were distinguished—confluent lysis, semiconfluent lysis, single plaques, growth inhibition, or no lysis. If single plaques appeared at any dilution, the strain was considered susceptible. (A) Phage-sensitive control strain RN4220 (pCN51) compared to wild-type phage resistant RN4220 ($53^+$) (pCN51) and RN4220 (pCN51-$pdp_{Sau}$) harboring $pdp_{Sau}$ gene on prophage 53 or plasmid pCN51, respectively. Phage 812a replicates effectively on strains with the $pdp_{Sau}$ gene. (B) *S. aureus* strains RN4220 ($53^+$) (pCN51-ORF812a_191) and RN4220 (pCN51-$pdp_{Sau}$-ORF812a_191) coexpressing $pdp_{Sau}$ and ORF 812a_191, which restores the sensitive phenotype. The restoration of the phage-sensitive phenotype occurs both in the lysogenic strain with prophage-encoded $pdp_{Sau}$ and the strain with coexpressed $pdp_{Sau}$ and ORF 812a_191 from a common promoter.

**The $pdp_{Sau}$ gene prevalence in *S. aureus* whole-genome sequences.** Analyses of the prevalence of $pdp_{Sau}$-encoding prophages in more than 60 thousand *Staphylococcaceae* genomes available in the NCBI database matched a set of 41 bacterial genomes with this gene. The $pdp_{Sau}$ gene was found solely on *S. aureus* prophage regions. A gene with lower similarity was found in the prophage genomes of coagulase-negative staphylococci and the genus *Aerococcus* (Fig. 2A). The extracted prophage sequences were classified by BLAST



Downloaded from https://journals.asm.org/journal/mbio on 08 August 2023 by 144.32.224.27.

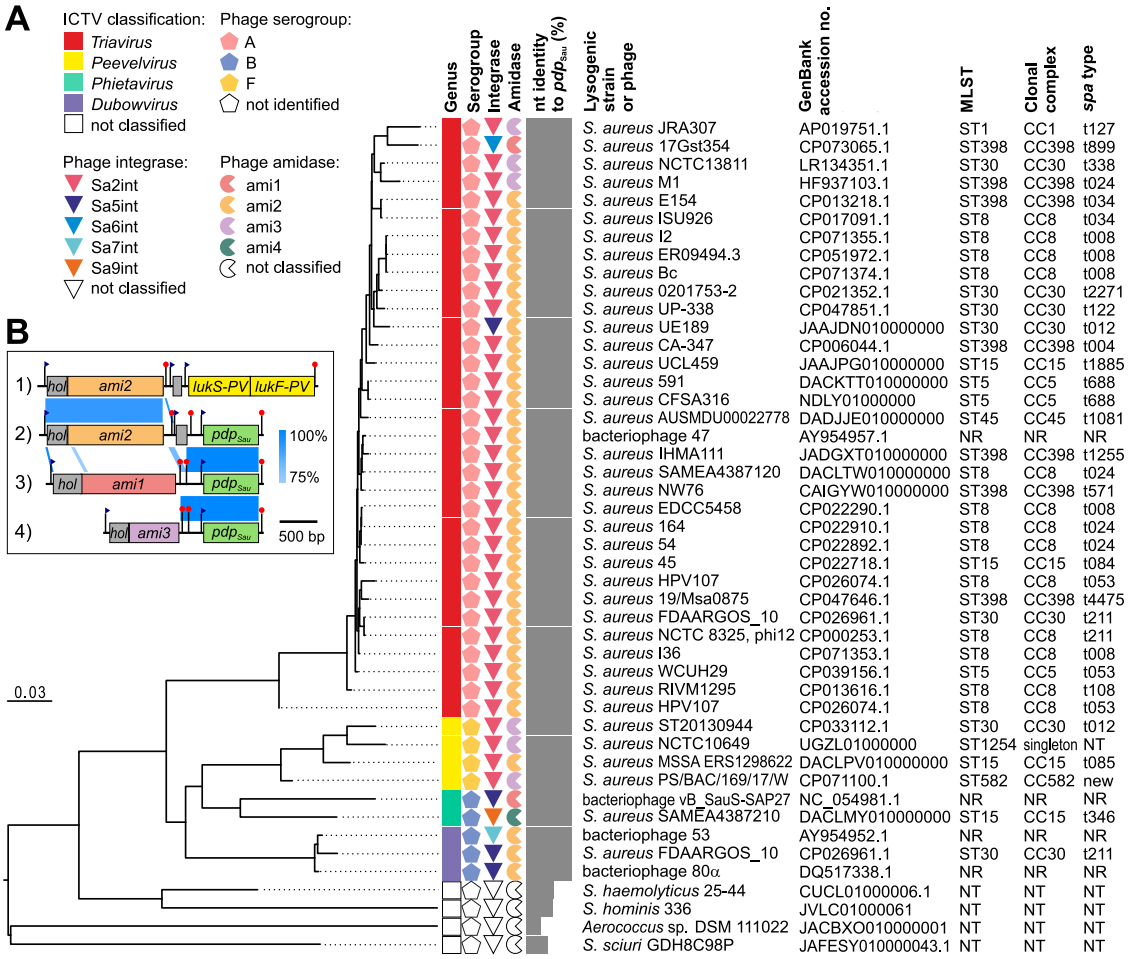


**FIG 2** Phylogenetic insights into prophages harboring *pdp*$_{Sau}$ gene identified in whole-genome sequences of *Staphylococcaceae* family and their characteristics. (A) Bacteriophage and prophage genomes extracted from whole-genome sequences that matched *pdp*$_{Sau}$ were compared using the Genome-BLAST Distance Phylogeny method with the settings recommended for prokaryotic viruses (90). The resulting intergenomic distances were used to infer a balanced minimum evolution tree with branch support via FASTME including Subtree Pruning and Regrafting (SPR) postprocessing (91). The branch lengths of the resulting tree are scaled in terms of the respective distance formula used. Phage genomes were characterized by phage type corresponding to serological group (65), integrase gene type (44), and amidase gene type (42). The nucleotide identity of *pdp*$_{Sau}$ homologs to ORF016 of phage 53 is shown. Multilocus sequence type and staphylococcal protein A (*spa*) type were derived from the genome assemblies. NR, not relevant; NT, not typeable. (B) Nucleotide sequence alignment showing the gene structure of lytic modules and accessory genes in the genomes of four *S. aureus* prophages as follows: (i) phi PVL (92), (ii) phi 53 (39), (iii) prophage vB_StaphS-IVBph354 (93), and (iv) prophage from strain PS/BAC/169/17/W (94). ORFs with proven or predicted functions are depicted as colored boxes. Nucleotide identity between genomic regions is indicated by blue-shaded regions. Putative promoters and terminators are depicted as blue flags and red pins, respectively.

search and *in silico* PCR into the genera *Triavirus*, *Phietavirus*, *Peevelvirus*, and/or *Dubowvirus* (Fig. 2A). The most frequent ones (85%) were prophages harboring Sa2 integrase, and the rest comprised integrase types Sa5, Sa6, Sa7, and Sa9. The gene organization of the lytic module shows that *pdp*$_{Sau}$ is always localized downstream of the gene for amidase in the lysis module (Fig. 2B) and is typically linked to amidase ami2 according to the previous classification system (42). The presence of the *pdp*$_{Sau}$ gene adjacent to ami2 was also confirmed by PCR in multiple lysogenic MRSA strain E48. The ami2 lytic module of *pdp*$_{Sau}$-positive phages was homologous with Panton-Valentine leukocidin (PVL)-converting phages (100% nucleotide [nt] identity) (Fig. 2B), which leads to the hypothesis that it has the same origin as in PVL-encoding phages (43). As determined previously (44), the crossover point for the integration of the PVL toxin-encoding complex is situated at the end of the phage amidase open reading frame (ORF), and the *pdp*$_{Sau}$ locus possibly recombines at this crossover point.

Next, we tested whether there was a relationship between the presence of the *pdp*$_{Sau}$ gene and clonal complexes of whole-genome sequenced lysogenic strains. Predominant genotypes from clonal complexes CC5, CC8, CC15, CC30, and ST398 (Fig. 2A) are typical



Downloaded from https://journals.asm.org/journal/mbio on 08 August 2023 by 144.32.224.27.

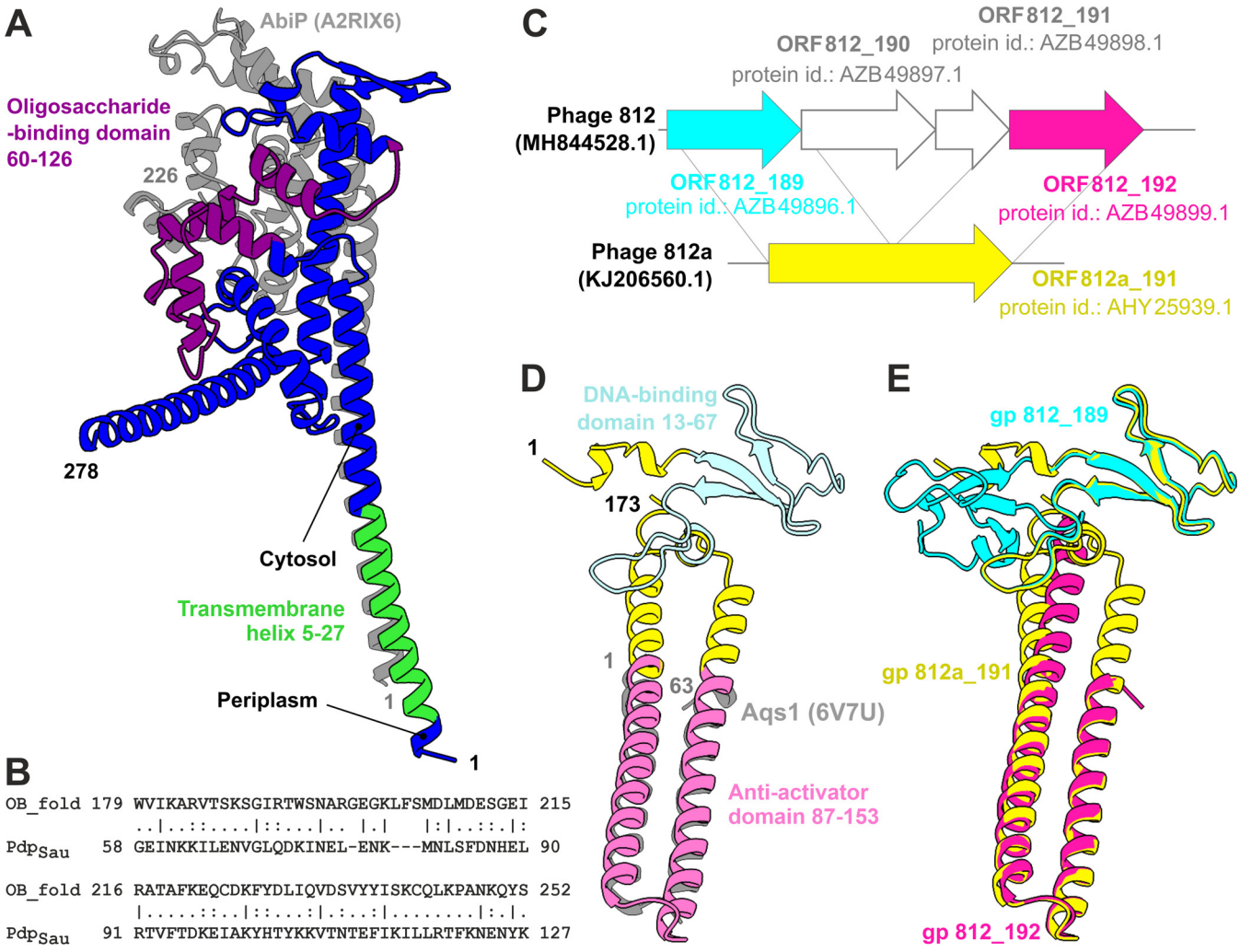


**FIG 3** Structure prediction of immunity protein $Pdp_{Sau}$ and new fusion protein restoring phage sensitivity encoded by phage mutant 812a. (A) 3D structure prediction of $Pdp_{Sau}$ (blue) with N-terminal transmembrane helix (lime green) and oligosaccharide-binding fold-like region (purple) highlighted. The structure is superimposed with the predicted structure of characterized immunity protein AbiP (A2RIX6) from *Lactococcus* (gray). (B) EMBOSS Needle pairwise alignment (BLOSUM62) of oligosaccharide-binding (OB) domains of RPA replication protein (UniProtKB accession no. Q24492) with OB_fold hit in $Pdp_{Sau}$ protein (score, 25; similarity, 40.5%). (C) Sequence alignment of genomic loci encoding ORF 812_189 and ORF 812_192 in phage 812 and fusion ORF 812a_191 in the genome of host-range mutant phage 812a, depicting the emerging deletion. (D) 3D structure prediction of fusion protein ORF812a_191, superimposed with the solved structure of the antiactivator Aqs1 (PDB accession no. 6V7U; gray). (E) Structural alignment of gene products encoded by ORF 812_189 (cyan), ORF 812_192 (magenta), and fusion ORF 812a_191 (yellow).

for community isolates where prophage-induced immunity to kayviruses may represent an evolutionary advantage, e.g., for survival and dissemination in a wastewater environment as an important reservoir for lytic phages (45).

**Transmembrane protein $Pdp_{Sau}$ is structurally similar to apoptotic protein.** Region 5 to 27 of the 278-amino acid (aa) protein $Pdp_{Sau}$ contains many hydrophobic residues and protein topology prediction classified it as a transmembrane domain (TMHMM, probability of N-in, 0.985) (Fig. 3A). Furthermore, structure comparison of the $Pdp_{Sau}$ protein region 3 to 28 suggests a weak similarity of the region to *Enterococcus faecalis* RNAI protein (2KV5) and *S. aureus* PepA1 protein (4B19) (see Table S1 in the supplemental material). RNAI forms part of the *par* locus and has the function of an Fst toxin for the stable maintenance of plasmids in cells (46). Fst translocated across a membrane induces changes in membrane integrity, leading to the disruption of cell division (47). PepA1 protein, similarly to Fst, forms a membrane-binding $\alpha$-helix in a 22-residue part of its N terminus (48). The liquid chromatography-tandem mass spectrometry (LC-MS/MS) analysis (see Table S2 in the supplemental material) revealed a predominant allocation of $Pdp_{Sau}$ protein in the membrane fraction compared to the cytoplasmic one; therefore, we assume $Pdp_{Sau}$ is embedded in the



Downloaded from https://journals.asm.org/journal/mbio on 08 August 2023 by 144.32.224.27.

membrane. The cytoplasmic C-terminal domain of $Pdp_{Sau}$ is positively charged. Pairwise sequence alignment (Fig. 3B) confirmed the presence of an oligosaccharide-binding fold (UniProtKB accession no. Q24492), which often facilitates DNA-binding function (49). Both transmembrane and DNA-binding domains were described in the lactococcal phage-defense abortive system protein AbiP (UniProtKB accession no. A2RIX6) (50). We thus compared protein models generated by Alphafold2 of $Pdp_{Sau}$ to AbiP, which despite the low amino acid identity exhibited a significant structural similarity demonstrated by their pairwise superimposing (Fig. 3A; see also Table S1).

Based on protein structure predictions, we hypothesize that $Pdp_{Sau}$ is one of the apoptotic-like membrane proteins associated with abortive systems (Abi), whose modes of action involve degradation or depolarization of the cell membrane (50). In Gram-positive bacteria, Abi systems provide resistance against phage infection that can lead to cell death and target various stages of the cell life cycle (50–52). Other classes of Abi systems target tRNAs or mRNAs and cleave essential proteins in the host translation apparatus, resulting in growth arrest and nonproductive infection (53), or compete with native replicase proteins (54).

**The *pdp*$_{Sau}$ gene does not affect *Kayvirus* adsorption and genome release but blocks its DNA replication.** To study the mechanism of action of $Pdp_{Sau}$, the strains RN4220, RN4220 ($53^{+}$), and RN4220 (pCN51-*pdp*$_{Sau}$) were infected with the wild-type phage 812. The reaction of strains to infection with phage was monitored by turbidity assay. Strains expressing *pdp*$_{Sau}$ exhibited growth of the bacterial culture upon infection with phage 812, which was slowed down for the first 4 h compared to uninfected culture, whereas the absence of the *pdp*$_{Sau}$ gene led to lysis of the culture (see Fig. S1 in the supplemental material). The expression level of the *pdp*$_{Sau}$ gene during phage 812 infection was determined using quantitative reverse transcription-PCR (RT-qPCR). Neither overexpression nor downregulation of the *pdp*$_{Sau}$ gene was detected at 0, 5, 10, and 20 min of infection with phage 812 compared to the sample without the addition of phage (see Table S3 in the supplemental material). The change in the expression of the *pdp*$_{Sau}$ gene is therefore not essential for the activation of the phage defense mechanism.

Next, we examined specific steps of the phage life cycle—adsorption, genome delivery, transcription, and replication—to determine at which point the cycle is arrested. The comparison of adsorption rate (see Fig. S2 in the supplemental material) showed that phage 812 virions adsorb efficiently onto both *pdp*$_{Sau}$-positive and -negative cells; thus, $Pdp_{Sau}$ does not affect adsorption.

We recently showed that *Kayvirus* transcription starts immediately after the entry of phage DNA into the host cells (26). To verify that *Kayvirus* phage 812 genome delivery and the transcription of its DNA occurs in *pdp*$_{Sau}$-positive *S. aureus* strains, the transcripts of the early (anti-sigma factor, orf 812_132; GenBank accession no. AZB49840.1), middle (putative DNA-binding protein, 812_143; GenBank accession no. AZB49851.1), and late (baseplate wedge protein, 812_118; GenBank accession no. AZB49826.1) phase of infection (26) were quantified by RT-qPCR (see Fig. S3 in the supplemental material). The presence of transcripts of all of the tested loci confirmed that the DNA of phage 812 is inside cells and accessible to the host transcription apparatus. Based on the facts that phage DNA is present inside the cell and $Pdp_{Sau}$ is structurally similar to lactococcal AbiP, we hypothesize that similarly to AbiP, the binding of a nucleic acid to $Pdp_{Sau}$ activates the phage resistance mechanism.

The replication of phage 812 was examined using the absolute quantification of the *mcp* gene for major capsid protein during infection (see Fig. S4 in the supplemental material). Rees and Fry in their original study of the phage K replisome (55) described that during the first half of the latent period, the number of phage DNA molecules increased from 1 copy to 27 phage equivalents. This observation is consistent with quantitative PCR (qPCR) results, where we detected about a 30-fold increase in the amount of phage 812 DNA in the sensitive control strain RN4220 20 min postinfection (Fig. S4). After 30 min, the copy number of the *mcp* gene increased about 40-fold in control RN4220 compared to those of *pdp*$_{Sau}$-positive strains, where the *mcp* copy number only increased 2-fold. The very low increase in the genome copy number leads to the presumption that the phage replication in *pdp*$_{Sau}$-positive strains is either not activated or is stalled at the very beginning.



Downloaded from https://journals.asm.org/journal/mbio on 08 August 2023 by 144.32.224.27.

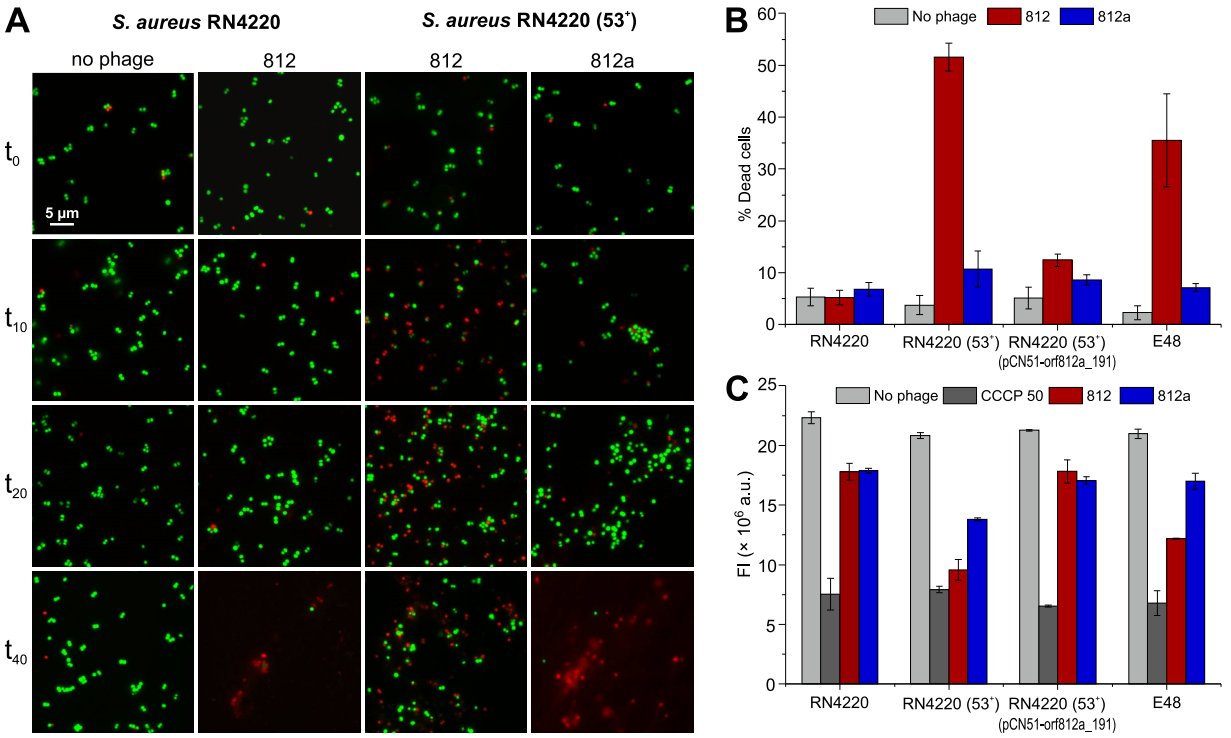


**FIG 4** Changes in *S. aureus* membrane permeability through $Pdp_{Sau}$-based phage defense mechanism illustrated by LIVE/DEAD staining. (A) Fluorescence microscopy of *S. aureus* infected with phages 812 or 812a and no phage control sample, visualized by fluorescence microscopy at time points 0, 10, 20, and 40 min after the onset of infection. Propidium iodide, a red-fluorescent nucleic acid-binding dye, which cannot enter cells with intact membranes, was used as a marker for the loss of membrane integrity and cell death. Dead cells are represented by red dots and live cells by green dots. (B) Percentage of dead bacterial cells 10 min after the onset of infection. *S. aureus* cultures were infected with phages 812 or 812a and compared with noninfected strains. (C) Changes in membrane polarity examined by BacLight bacterial membrane potential kit assay on *S. aureus* RN4220, RN4220 ($53^+$), RN4220 ($53^+$) (pCN51-orf812a_191), and clinical MRSA strain E48 treated with phages 812 or 812a at an $MOI_{input}$ of 10. Treatment with the ionophore carbonyl cyanide 3-chlorophenylhydrazone, component B (CCCP) at a final concentration of 50 mM was used as a positive control of depolarization. The decrease in membrane potential was measured as a loss of red fluorescence emitted by carbocyanine dye $DiOC_2(3)$ (3,3′-diethyloxa-carbocyanine iodide).

***$pdp_{Sau}$* impacts cell membrane potential and permeability in *Kayvirus*-infected cells.** Due to the assumed transmembrane localization of $Pdp_{Sau}$ protein, the changes in the cell membrane integrity 10 to 40 min postinfection in strains RN4220 and RN4220 ($53^+$) were assessed using LIVE/DEAD cell staining. In the RN4220 strain, we observed live cells until the release of new phage progeny after 40 min (Fig. 4A). Compared to the *$pdp_{Sau}$* gene-negative strain RN4220, we observed a presence of dead cells 10 min postinfection and subsequent increase in cell counts with no cell lysis after 40 min postinfection in *$pdp_{Sau}$* gene-positive strain RN4220 ($53^+$) (Fig. 4A and B). This indicates halted phage propagation followed by a rapid growth of live cells starting from 20 min after infection (Fig. 4A). In this way, the bacterial population survives due to an abortive defense mechanism.

Changes in membrane permeability are connected with membrane potential. The carbocyanine dye staining showed a statistically significant reduction in red fluorescence ($P$ value $< 0.01$) in the *$pdp_{Sau}$*-negative nonlysogenic strain RN4220 compared to that in the *$pdp_{Sau}$*-positive lysogenic strain RN4220 ($53^+$), indicating a change in membrane potential (Fig. 4C). This was also observed in the control MRSA strain E48 (Fig. 4B and C). Similarly, the abortive Rex system of bacteriophage lambda characterized by termination of macromolecular synthesis, loss of active transport, ATP hydrolysis, and altruistic cell death is explained by depolarization of the cytoplasmic membrane due to activation of the membrane component of the system (56).

**Kayviruses can escape prophage-induced bacterial resistance mechanism.** Bacteriophage 812 host-range mutants are capable of growing on *$pdp_{Sau}$*-positive strains. This capability was first observed in a mutant designated 812a, which was obtained as rare plaques after plating phage 812 (mutation frequency, $9.9 \times 10^{-9}$; efficiency of plating, 0.43)



Downloaded from https://journals.asm.org/journal/mbio on 08 August 2023 by 144.32.224.27.

on the lysogenic strain *S. aureus* NCTC 8511 (53$^+$) (38). Phage 812a propagated efficiently on all of the analyzed lysogenic $pdp_{Sau}$-positive strains, as determined by phage drop plaque assays (Table 1; Fig. 1A), turbidity assay (Fig. S1), and microscopic observation of the infected cells (Fig. 4A).

Whole-genome sequencing of phage 812a (15) revealed a deletion leading to a new fusion gene with a possible role in overcoming the action of $Pdp_{Sau}$. The deletion in phage 812 genome includes a locus encoding four hypothetical genes (ORF 812_189 to ORF 812_192; GenBank accession no. MH844528.1). After the deletion, ORF 812_189 and ORF 812_192 form a fusion gene in phage 812a annotated as ORF 812a_191 (GenBank accession no. KJ206560.1) (Fig. 3C and E). The new 173-aa fusion protein has a conserved DNA-binding domain on its N terminus (residues 13 to 67) with a zinc finger motif similar to Miz-1 protein (HHpred, 2N26; probability, 98.81%; e value, 6.4e−9) (57) and to the transcription repressor CTCF from eukaryotes (HHpred, 6QNX, probability: 98.4%, e-value 1.4e−7) (58). The tertiary structure of the protein in the C-terminal region 87 to 153 is similar to the antiactivator Aqs1 of *Pseudomonas* phage DSM3 (DALI search, PDB accession no. 6V7U; Z-score = 6.5) (Fig. 3D), which is involved in blocking a host phage-resistance mechanism by inhibiting the DNA-binding domain of a host cell regulator (59).

To verify the direct association of the new fusion gene with overcoming the resistance mechanism, ORF 812a_191 was coexpressed with $pdp_{Sau}$ under one promoter in *S. aureus* RN4220 (pCN51-$pdp_{Sau}$-orf812a_191), which led to restored sensitivity to phages 812 and K. The same phenomenon was confirmed in the *S. aureus* RN4220 (53$^+$) (pCN51-orf812a_191) system, which naturally carries $pdp_{Sau}$ in the genome (Fig. 1B; see also Fig. S1). No change in membrane potential or permeability was observed when *S. aureus* strain RN4220 (53$^+$) (pCN51-orf812a_191) was infected with phage 812 (Fig. 4B and C).

**Conclusions.** The described defense mechanism encoded by a prophage accessory gene protects the staphylococcal bacterial population against virulent lytic phages via abortive infection. Because it is encoded by prophages in various clonal lineages, we assume it was spread by horizontal gene transfer. An analogy can be found in the abortive mechanisms of lactococci (53) but even in a group of Gram-negative bacteria (60), where the responsible genes are also carried by mobile genetic elements. The interaction of the prophage gene product with the infecting phage halts the replication of its DNA and leads to changes in the permeability of the cell membrane. Based on these findings, we conclude that the infected part of the bacterial host population is sacrificed to stop the lytic infection by the *Kayvirus* and prevent the release of its new progeny. The bacteria benefit from a lysogenic conversion that allows them to escape the lytic action of *Kayvirus* at the population level. Therefore, we believe that this novel mechanism of phage competition in staphylococci leads to the stable maintenance of prophages protecting their hosts. Kayviruses can evolve through mutations and regain the ability to lyse lysogenic strains, thus maintaining their wide range of hosts, which is important for their use in phage therapy.

## MATERIALS AND METHODS

**Bacterial and bacteriophage strains and culture conditions.** The strains used in this study are listed in Table 1. Staphylococcal strains were routinely grown in meat peptone broth (MPB) and/or meat peptone agar (MPA) according to Botka et al. (15). *Escherichia coli* strains were grown at 37°C with shaking at 160 rpm in LB medium. Phage 812, deposited in the Czech Collection of Microorganisms under number CCM 7911, and phage 812a were described previously (38). Bacteriophage K was kindly provided by G. Xia (University of Manchester, UK) (61). *S. aureus* phages from the International Typing Set (62) and phage 80$\alpha$ (63) were described previously. Lysogenized strains were prepared as previously described (64), and the presence of prophages was verified by PCR (65). The phage-cured *S. aureus* strain USA300 (designated USA300c) was generated by deleting native prophages $Sa2int_{USA300}$ and $Sa3int_{USA300}$ using the plasmid pKOR1 as described for *S. aureus* Newman (66). Phage-cured strains ISP8 (53$^+$)c and NCTC 8511 (53$^+$)c were prepared by using UV light and recognized by replica plating on MPA medium inoculated with an indicator strain (64).

**Construction of plasmid vectors and protein preparation.** The expression vectors constructed in this study are derived from high-copy-number shuttle vector plasmid pCN51 with cadmium-inducible promoter (41) and are listed in Table 1. The protein-coding regions were amplified by PCR with primers designed for restriction enzyme cloning (see Table S4 in the supplemental material). Restriction endonucleases BamHI and EcoRI (New England Biolabs) were used for cloning by ligation with T4 DNA ligase (New England Biolabs). Plasmid constructs were transformed into competent *E. coli* Top10F′ (Invitrogen) and then into *E. coli* BL21(DE3) (Invitrogen) for protein expression or transferred into electrocompetent *S. aureus* cells (67). All constructs were verified by



Downloaded from https://journals.asm.org/journal/mbio on 08 August 2023 by 144.32.224.27.

Sanger sequencing in the Eurofins MWG Operon sequencing facility (Ebersberg, Germany). The expression and coexpression of cloned genes from plasmid constructs were verified by mass spectrometry.

**Phage susceptibility testing.** The double agar overlay technique (MPA with 2 mM $CaCl_2$) was used for phage susceptibility testing and the isolation of phage mutants. The phage lysates of a titer of $10^9$ PFU/mL were diluted up to $10^{-6}$ and applied in triplicates by spotting 10-$\mu$L aliquots onto soft agar lawns inoculated with the tested *S. aureus* strain. Plates were incubated overnight at 37°C. The strain was only evaluated as sensitive if the phage formed plaques.

**Adsorption assays.** The adsorption efficiency of phages 812 and 812a onto *S. aureus* strains RN4220 and RN4220 ($53^+$) was determined as described previously (33). Briefly, the adsorption was analyzed using a multiplicity of infection ($MOI_{input}$) of 0.1, and the adsorption rate (%) was calculated by determining the number of unbound phage particles in the supernatant and subtracting it from the total number of input PFU as a ratio of the total number of input PFU. The adsorption rate was estimated 5 min after phage infection.

**Bacterial cell growth assays during phage infection.** Bacterial strains were cultivated aerobically in 20 mL of MPB to the logarithmic phase (optical density at 600 nm [$OD_{600}$] = 0.4 to 0.45) at 37°C. A transparent 96-well cell culture plate (SPL Life Sciences) with a transparent cover and an Infinite 200 PRO (Tecan) microplate reader were used for the turbidimetric assay. The experiments were carried out in triplicates in a total volume of 200 $\mu$L per well at 37°C with continuous orbital shaking (amplitude, 4 mm) for 24 h using the recommended protocol and instrument settings (absorbance, 600 nm; 20 flashes; 0 ms settle time). Phage infection assay was done at an $MOI_{input}$ of 5 or 10 with the addition of $CaCl_2$ to a final concentration of 2 mM.

**DNA extraction for phage gene quantification in infected cells.** Bacterial culture grown to an $OD_{600}$ of 0.4 to 0.45 in 50 mL MPB at 37°C was mixed with phages 812 or 812a at an $MOI_{input}$ of 0.1 and incubated with shaking. The 1.5-mL aliquots were taken at sampling time points 0, 2, 5, 10, 15, 20, and 30 min and centrifuged at 10,000 $\times$ *g* for 2 min. Pellets were frozen using liquid nitrogen and kept at −80°C. DNA was extracted from each aliquot sample using a High Pure PCR template preparation kit (Roche) with prolonged lysis with lysostaphin (Sigma-Aldrich) added to a final concentration of 10 $\mu$g/mL.

**cDNA preparation.** Total RNA was extracted using the TRI reagent (Sigma-Aldrich) from *S. aureus* cells infected with phages at sampling time points 0, 2, 5, 10, 15, 20, and 30 min, harvested as described above. The procedure was done in RNase-free tubes according to the manufacturer's instructions with the following modifications for the lysis of Gram-positive bacteria: $10^8$ cells were lysed in 1 mL of TRI reagent and transferred to lysing matrix B with 0.1 mm silica spheres (MP Biomedicals) and homogenized for 2 min. The silica spheres were collected by centrifugation for 3 min at 10,000 $\times$ *g* at 4°C. Purified RNA was used for cDNA synthesis in a reverse transcription assay using a high-capacity cDNA reverse transcription kit (Applied Biosystems).

**qPCR and RT-qPCR of phage genes at different times of infection.** Each reaction mixture (20 $\mu$L) contained 10 $\mu$L of 2$\times$ LightCycler 480 SYBR green I master (Roche), forward and reverse primers (each 10 $\mu$M) listed in Table S4, and template DNA or cDNA diluted into a volume of 5 $\mu$L. Reactions were carried out in triplicates using a LightCycler 480 Instrument II (Roche) according to Mašlaňová et al. (68). An initial denaturation of DNA at 95°C for 10 min was followed by 30 cycles of amplification (95°C for 15 s, 55°C for 20 s, 72°C for 15 s) and a dissociation phase at 95°C for 15 s, 60°C for 60 s, 95°C for 5 s, and 60°C for 15 s. The amplification efficiency of qPCR was calculated from threshold cycle ($C_T$) values of standard curves prepared from the plasmid or genomic DNA for each reaction, and a linear regression curve through the data points was generated. The measurements were done in biological and technical triplicates. The expression level was analyzed from crossing point (Cp) values using a one-way analysis of variance (ANOVA) test. All statistical analyses were performed in R v4.2.1. (https://cran.r-project.org/).

**Protein identification by mass spectrometry.** Vertical one-dimensional SDS-PAGE was performed as described previously (69). Separation zones corresponding to the molecular weight of the expected protein (33 $\pm$ 5 kDa) were excised from the gel, and after destaining and washing procedures, they were digested with trypsin (Promega) for 2 h at 40°C. Tryptic peptides extracted from gels were subjected to LC-MS/MS analysis using an UltiMate 3000 RSLCnano liquid chromatography system (Thermo Fisher Scientific) connected on-line to an Impact II ultra-high resolution Qq-time-of-flight mass spectrometer (Bruker, Germany). MS/MS data were searched against a custom database of expected amino acid sequences and in parallel against the NCBIprot database (https://ftp.ncbi.nih.gov/blast/db/FASTA/) using an in-house Mascot search engine version 2.4.1 (Matrix Science, UK).

To obtain cytoplasmic (C) and membrane (M) protein fractions, the isolation method described previously (70) was used with changes for the final processing of the membrane fraction. The pelleted membrane fraction was washed twice with 50 mM ammonium bicarbonate (AB), centrifuged at 20,000 $\times$ *g* for 10 min, and solubilized in SDT lysis buffer (4% SDS, 0.1 M dithiothreitol, 0.1 M Tris-HCl, pH 7.6). Solubilized proteins were processed using filter-aided sample preparation (FASP) and digested with SOLu-trypsin dimethylated (Merck) in 50 mM AB. Recovered peptides were cleaned using ethyl acetate extraction. LC-MS/MS analyses of both fractions were performed in an RSLCnano liquid chromatography system on-line connected to an Orbitrap Exploris 480 mass spectrometer (Thermo Fisher Scientific). Peptides were separated using an analytical EASY-Spray column (Acclaim PepMap $C_{18}$ column; 2-$\mu$m particles, 75 $\mu$m $\times$ 500 mm; Thermo Fisher Scientifics; part number ES903) during a 138-min gradient elution (mobile phase A, 0.1% formic acid in water; mobile phase B, 0.1% formic acid in 80% acetonitrile). MS data were acquired in a data-dependent strategy with a defined number of scans based on precursor abundance with survey scan (*m/z* 350 to 2,000). The resolution of the survey scan was 120,000 (at *m/z* 200) with a target value of $1 \times 10^6$ ions and maximum injection time of 500 ms. High-energy collisional dissociation-tandem mass spectrometry (HCD-MS/MS) data (30% relative fragmentation energy) were recorded at 15,000 resolution (maximum injection time, 50 ms). MaxQuant software version 2.0.3.0 with inbuild search engine Andromeda (Max-Planck-Institute of Biochemistry) was used for data evaluation. Searches were done against the *S. aureus* NCTC 8325 reference proteome (UP000008816) and cRAP contaminants database version 2012.01.01. Carbamidomethylation of cysteine was set as a fixed modification while oxidation (M), deamidation



Downloaded from https://journals.asm.org/journal/mbio on 08 August 2023 by 144.32.224.27.

(N, Q), and acetylation (protein N-term) were set as variable modifications. Trypsin was used as the protein-cleaving enzyme with two allowed missed cleavages. Peptides and proteins with a false discovery rate of <1% were considered for final data evaluation. All identified proteins including the protein of interest (UniProtKB accession no. Q2FYE0) are listed in Table S2 in the supplemental material. Mass spectrometry data were deposited in the ProteomeXchange Consortium via the PRIDE partner repository under database identifier PXD036676.

**Bacterial membrane permeability and membrane polarity assays.** *S. aureus* strains RN4220, RN4220 ($53^+$), RN4220 ($53^+$) (pCN51-orf812a_191), and E48 were routinely grown in MPB. The bacterial culture was 100-fold diluted in MPB supplemented with 0.5 $\mu$M $Cd(NO_3)_2$ to induce expression where needed and incubated at 37°C with shaking to an $OD_{600}$ of 0.35 to 0.40. The phage 812 or 812a was added at an $MOI_{input}$ of 5. The bacterial cells without phages were used as a negative control. The 1.5-mL aliquots were taken at sampling times 0, 10, 20, and 40 min, centrifuged at 10,000 $\times$ *g* for 2 min, and the pellets were washed once and resuspended in 150 $\mu$L of 50 mM Tris-HCl (pH 7.5) for membrane permeability assay and in 150 $\mu$L of phosphate-buffered saline (PBS) buffer for membrane polarity assay. The cell suspension was stained using a LIVE/DEAD BacLight bacterial viability kit (Invitrogen) as recommended by the manufacturer. The kit contains SYTO 9 and propidium iodide (PI), which have different permeabilities through the bacterial membrane. The stained bacterial samples were observed with an Olympus BX41 fluorescence microscope (Olympus, Japan). The SYTO 9 emission was observed using a fluorescein isothiocyanate (FITC) filter cube (U-MWB2; excitation 475 $\pm$ 30 nm; emission >520 nm; dichroic mirror (DM) 500 nm) and the PI using a tetramethyl rhodamine isocyanate (TRITC) filter cube (U-MWG2; excitation 530 $\pm$ 40 nm; emission >590 nm; DM 570 nm). The measurements were done in biological and technical triplicates.

Changes in membrane polarity were detected with a BacLight bacterial membrane potential kit (Invitrogen) containing carbocyanine dye $DiOC_2(3)$ (3,3′-diethyloxa-carbocyanine iodide) and compared with the control ionophore carbonyl cyanide 3-chlorophenylhydrazone, component B (CCCP) at a final concentration of 50 $\mu$M, both diluted in dimethyl sulfoxide (DMSO). The precipitation of $DiOC_2(3)$ indicates changes in potential at the bacterial membrane, and its natural green emission shifts to red (71). The decrease in membrane potential was observed as a loss of red fluorescence using an Upcon S-Pro reader (Labrox, Finland) in a black nonbinding 96-well microplate (Greiner, Austria). Kinetic measurements were performed from the addition of ionophores for 1 h, and the intensity value was evaluated at 20 min. The filters used in this case were 485 $\pm$ 10 nm for excitation and 616 $\pm$ 8.5 nm for emission (DM excitation, 450 to 492 nm; emission, 520 to 550 nm). The measurements were done in biological and technical triplicates. The effect of phage addition on membrane depolarization in the tested strains was analyzed using analysis of variance (ANOVA) followed by *post hoc* Tukey tests performed in R v4.2.1.

**Protein structure prediction.** The transmembrane domain of $Pdp_{Sau}$ was predicted using TMHMM version 2.0 (72). The DNA-binding domain in $Pdp_{Sau}$ was predicted using DRNApred (73). HHpred (74), Phyre2 (75), and DALI search (76) were used for $Pdp_{Sau}$, estimating the similarity to distantly related proteins based on the secondary and tertiary structure prediction. The three-dimensional (3D) models of $Pdp_{Sau}$ and orf812a_191 protein structures were predicted by AlphaFold, developed by DeepMind (77). Chimera version 1.15.rc (78) and ChimeraX version 1.2.5 (79) were used for the visualization of 3D protein structures.

**Whole-genome sequencing.** The bacterial culture was prepared and enzymatically treated as previously described (80). The genomic DNA was extracted using a Genomic DNA Clean & Concentrator-25 kit (Zymo Research) according to the manufacturer's instructions. For sequencing on the Oxford Nanopore platform, the library was prepared using an SQK-RAD004 rapid sequencing kit (Oxford Nanopore Technologies) according to the manufacturer's instructions. The library was sequenced with a FLO-FLG001 flow cell (R9.4.1) in a MinION device (Oxford Nanopore Technologie). The device was controlled with MinION software release 22.05.5 (Oxford Nanopore Technologies). Basecalling, demultiplexing, and barcode trimming were performed using standalone ONT Guppy software version 6.1.7 using the config file dna_r9.4.1_450bps_sup.cfg with a default minimum q-score threshold of 10. For Illumina-based sequencing, the 500-bp sequencing library was prepared with an xGen DNA Lib Prep EZ (Integrated DNA Technologies, Belgium). The samples were sequenced using a 600v3 Miseq sequencing cartridge in a 2 $\times$ 300 paired end mode using an Illumina MiSeq sequencing platform (Illumina). Illumina reads were trimmed and filtered using Trimmomatic version 0.38.1 with the sliding window model using average quality required 20 (81). The complete bacterial genome sequence was obtained using a hybrid assembly with Unicycler version 0.4.8 (82) using a minimal k-mer size of 0.2 and highest k-mer size of 0.95 with 10 k-mer steps used in a SPAdes assembly. The resulting assembly was polished with Pilon version 1.24 (83). The genome was annotated using the NCBI Prokaryotic Genome Annotation Pipeline (84).

**Genomic sequences used in this study and bioinformatic analyses.** Whole genomic sequences with the $pdp_{Sau}$ gene were identified by BLAST search (https://blast.ncbi.nlm.nih.gov/). Prophage sequences from this data set were extracted manually based on their integration sites (42). The PubMLST website was used for multilocus sequence type (MLST) determination (85). Spa-types were derived with RIDOM Spa server (86). Phage and prophage genomes were characterized based on *in silico* PCR (87) using primers targeting structural genes corresponding to the serological group (65), integrase gene type (44), and amidase genes (42). Promoter sequences were predicted using the BPROM webserver (88), and terminator sites were predicted using ARNold (89).

**Data availability.** The complete genome sequence of *S. aureus* strain E48 (=NRL 02/947) has been deposited in GenBank/ENA/DDBJ under accession numbers CP103850 (chromosome) and CP103849 (plasmid). The associated BioProject and BioSample accession numbers are PRJNA873286 and SAMN30496472, respectively.

## SUPPLEMENTAL MATERIAL

Supplemental material is available online only.

**FIG S1**, PDF file, 1.3 MB.



Downloaded from https://journals.asm.org/journal/mbio on 08 August 2023 by 144.32.224.27.

**FIG S2**, PDF file, 1.3 MB.
**FIG S3**, PDF file, 1.3 MB.
**FIG S4**, PDF file, 1.3 MB.
**TABLE S1**, XLSX file, 0.01 MB.
**TABLE S2**, XLSX file, 2.6 MB.
**TABLE S3**, XLSX file, 0.02 MB.
**TABLE S4**, XLSX file, 0.01 MB.

## ACKNOWLEDGMENTS

This work was supported by a National Institute of Virology and Bacteriology project (Program EXCELES, ID project no. LX22NPO5103) funded by the European Union - Next Generation EU, a grant (18-13064S) from the Czech Science Foundation to R.P., grants (NU22-05-00042 and NU21J-05-00035) from the Ministry of Health of the Czech Republic to I.M. and T.B., respectively, a project from the Grant Agency of Masaryk University (MUNI/A/1325/2021) to J.D., and Wellcome Trust grant 224067/Z/21/Z to P.B.

We gratefully acknowledge the CIISB, Instruct-CZ Centre of Instruct-ERIC EU consortium, and the NCMG research infrastructure funded by the Ministry of Education, Youth and Sports of the Czech Republic (LM2018127) and European Regional Development Fund-Project "UP CIISB" (no. CZ.02.1.01/0.0/0.0/18_046/0015974) for their financial support of the measurements at the Proteomics, Nanobiotechnology, and Cryo-electron Microscopy and Tomography Core Facilities of CEITEC MU. The computational resources were supplied by the project e-INFRA CZ funded by the Ministry of Education, Youth and Sports of the Czech Republic (LM2018140).

We thank P. Formanová (Faculty of Science, Masaryk University) for valuable help with the pilot experiments. We thank C. Wolz (Interfaculty Institute of Microbiology and Infection Medicine, University of Tübingen) for providing the delysogenized *S. aureus* USA300c strain.

## REFERENCES

1. Suttle CA. 2007. Marine viruses-major players in the global ecosystem. Nat Rev Microbiol 5:801–812. https://doi.org/10.1038/nrmicro1750.
2. Feiner R, Argov T, Rabinovich L, Sigal N, Borovok I, Herskovits AA. 2015. A new perspective on lysogeny: prophages as active regulatory switches of bacteria. Nat Rev Microbiol 13:641–650. https://doi.org/10.1038/nrmicro3527.
3. Humphrey S, Fillol-Salom A, Quiles-Puchalt N, Ibarra-Chavez R, Haag AF, Chen J, Penadés JR. 2021. Bacterial chromosomal mobility via lateral transduction exceeds that of classical mobile genetic elements. Nat Commun 12:6509. https://doi.org/10.1038/s41467-021-26004-5.
4. Naorem RS, Goswami G, Gyorgy S, Fekete C. 2021. Comparative analysis of prophages carried by human and animal-associated *Staphylococcus aureus* strains spreading across the European regions. Sci Rep 11:18994. https://doi.org/10.1038/s41598-021-98432-8.
5. Ingmer H, Gerlach D, Wolz C. 2019. Temperate phages of *Staphylococcus aureus*. Microbiol Spectr 7:7.5.1. https://doi.org/10.1128/microbiolspec.GPP3-0058-2018.
6. Novick RP. 2003. Mobile genetic elements and bacterial toxinoses: the superantigen-encoding pathogenicity islands of *Staphylococcus aureus*. Plasmid 49:93–105. https://doi.org/10.1016/S0147-619X(02)00157-9.
7. Fillol-Salom A, Alsaadi A, Sousa JAM, Zhong L, Foster KR, Rocha EPC, Penades JR, Ingmer H, Haaber J. 2019. Bacteriophages benefit from generalized transduction. PLoS Pathog 15:e1007888. https://doi.org/10.1371/journal.ppat.1007888.
8. Haaber J, Leisner JJ, Cohn MT, Catalan-Moreno A, Nielsen JB, Westh H, Penadés JR, Ingmer H. 2016. Bacterial viruses enable their host to acquire antibiotic resistance genes from neighbouring cells. Nat Commun 7:13333. https://doi.org/10.1038/ncomms13333.
9. Mašlaňová I, Stříbná S, Doškař J, Pantůček R. 2016. Efficient plasmid transduction to *Staphylococcus aureus* strains insensitive to the lytic action of transducing phage. FEMS Microbiol Lett 363:fnw211. https://doi.org/10.1093/femsle/fnw211.
10. Łobocka M, Hejnowicz MS, Dąbrowski K, Gozdek A, Kosakowski J, Witkowska M, Ulatowska MI, Weber-Dąbrowska B, Kwiatek M, Parasion S, Gawor J, Kosowska H, Głowacka A. 2012. Genomics of staphylococcal Twort-like phages-potential therapeutics of the post-antibiotic era. Adv Virus Res 83:143–216. https://doi.org/10.1016/B978-0-12-394438-2.00005-0.
11. Hrebík D, Štveraková D, Škubník K, Füzik T, Pantůček R, Plevka P. 2019. Structure and genome ejection mechanism of *Staphylococcus aureus* phage P68. Sci Adv 5:eaaw7414. https://doi.org/10.1126/sciadv.aaw7414.
12. Petrovic Fabijan A, Lin RCY, Ho J, Maddocks S, Ben Zakour NL, Iredell JR, Westmead Bacteriophage Therapy Team. 2020. Safety of bacteriophage therapy in severe *Staphylococcus aureus* infection. Nat Microbiol 5:465–472. https://doi.org/10.1038/s41564-019-0634-z.
13. O'Flaherty S, Coffey A, Edwards R, Meaney W, Fitzgerald GF, Ross RP. 2004. Genome of staphylococcal phage K: a new lineage of Myoviridae infecting gram-positive bacteria with a low G+C content. J Bacteriol 186:2862–2871. https://doi.org/10.1128/JB.186.9.2862-2871.2004.
14. Ajuebor J, Buttimer C, Arroyo-Moreno S, Chanishvili N, Gabriel E, O'Mahony J, McAuliffe O, Neve H, Franz C, Coffey A. 2018. Comparison of Staphylococcus phage K with close phage relatives commonly employed in phage therapeutics. Antibiotics 7:37. https://doi.org/10.3390/antibiotics7020037.
15. Botka T, Pantůček R, Mašlaňová I, Benešík M, Petráš P, Růžičková V, Havlíčková P, Varga M, Žemličková H, Koláčková I, Florianová M, Jakubů V, Karpíšková R, Doškař J. 2019. Lytic and genomic properties of spontaneous host-range Kayvirus mutants prove their suitability for upgrading phage therapeutics against staphylococci. Sci Rep 9:5475. https://doi.org/10.1038/s41598-019-41868-w.
16. Sáez Moreno D, Visram Z, Mutti M, Restrepo-Cordoba M, Hartmann S, Kremers AI, Tišáková L, Schertler S, Wittmann J, Kalali B, Monecke S, Ehricht R, Resch G, Corsini L. 2021. $\varepsilon^2$-Phages are naturally bred and have a vastly improved host range in *Staphylococcus aureus* over wild type phages. Pharmaceuticals (Basel) 14:325. https://doi.org/10.3390/ph14040325.
17. Sanz-Gaitero M, Keary R, Garcia-Doval C, Coffey A, van Raaij MJ. 2013. Crystallization of the CHAP domain of the endolysin from *Staphylococcus aureus* bacteriophage K. Acta Crystallogr Sect F Struct Biol Cryst Commun 69:1393–1396. https://doi.org/10.1107/S1744309113030133.
18. Benešík M, Novaček J, Janda L, Dopitová R, Pernisová M, Melková K, Tišáková L, Doškař J, Žídek L, Hejátko J, Pantůček R. 2018. Role of SH3b binding domain in a natural deletion mutant of Kayvirus endolysin LysF1 with a broad range of lytic activity. Virus Genes 54:130–139. https://doi.org/10.1007/s11262-017-1507-2.
19. Horgan M, O'Flynn G, Garry J, Cooney J, Coffey A, Fitzgerald GF, Ross RP, McAuliffe O. 2009. Phage lysin LysK can be truncated to its CHAP domain



Downloaded from https://journals.asm.org/journal/mbio on 08 August 2023 by 144.32.224.27.

and retain lytic activity against live antibiotic-resistant staphylococci. Appl Environ Microbiol 75:872–874. https://doi.org/10.1128/AEM.01831-08.
20. Simon K, Pier W, Kruttgen A, Horz HP. 2021. Synergy between phage Sb-1 and oxacillin against methicillin-resistant *Staphylococcus aureus*. Antibiotics 10:849. https://doi.org/10.3390/antibiotics10070849.
21. Kaźmierczak Z, Majewska J, Miernikiewicz P, Międzybrodzki R, Nowak S, Harhala M, Lecion D, Kęska W, Owczarek B, Ciekot J, Drab M, Kędzierski P, Mazurkiewicz-Kania M, Górski A, Dąbrowska K. 2021. Immune response to therapeutic staphylococcal bacteriophages in mammals: kinetics of induction, immunogenic structural proteins, natural and induced antibodies. Front Immunol 12:639570. https://doi.org/10.3389/fimmu.2021.639570.
22. Nováček J, Šiborová M, Benešík M, Pantůček R, Doškař J, Plevka P. 2016. Structure and genome release of Twort-like Myoviridae phage with a double-layered baseplate. Proc Natl Acad Sci U S A 113:9351–9356. https://doi.org/10.1073/pnas.1605883113.
23. Zelasko S, Górski A, Dabrowska K. 2017. Delivering phage therapy *per os*: benefits and barriers. Expert Rev Anti Infect Ther 15:167–179. https://doi.org/10.1080/14787210.2017.1265447.
24. Kifelew LG, Warner MS, Morales S, Vaughan L, Woodman R, Fitridge R, Mitchell JG, Speck P. 2020. Efficacy of phage cocktail AB-SA01 therapy in diabetic mouse wound infections caused by multidrug-resistant *Staphylococcus aureus*. BMC Microbiol 20:204. https://doi.org/10.1186/s12866-020-01891-8.
25. Leskinen K, Tuomala H, Wicklund A, Horsma-Heikkinen J, Kuusela P, Skurnik M, Kiljunen S. 2017. Characterization of vB_SauM-fRuSau02, a Twort-like bacteriophage isolated from a therapeutic phage cocktail. Viruses 9:258. https://doi.org/10.3390/v9090258.
26. Finstrlová A, Mašlaňová I, Blasdel Reuter BG, Doškař J, Götz F, Pantůček R. 2022. Global transcriptomic analysis of bacteriophage-host interactions between a Kayvirus therapeutic phage and *Staphylococcus aureus*. Microbiol Spectr 10:e00123-22. https://doi.org/10.1128/spectrum.00123-22.
27. Arroyo-Moreno S, Buttimer C, Bottacini F, Chanishvili N, Ross P, Hill C, Coffey A. 2022. Insights into gene transcriptional regulation of *Kayvirus* bacteriophages obtained from therapeutic mixtures. Viruses 14:626. https://doi.org/10.3390/v14030626.
28. Eyer L, Pantůcek R, Zdráhal Z, Konecná H, Kaspárek P, Růzicková V, Hernychová L, Preisler J, Doskar J. 2007. Structural protein analysis of the polyvalent staphylococcal bacteriophage 812. Proteomics 7:64–72. https://doi.org/10.1002/pmic.200600280.
29. Dy RL, Richter C, Salmond GP, Fineran PC. 2014. Remarkable mechanisms in microbes to resist phage infections. Annu Rev Virol 1:307–331. https://doi.org/10.1146/annurev-virology-031413-085500.
30. van Houte S, Buckling A, Westra ER. 2016. Evolutionary ecology of prokaryotic immune mechanisms. Microbiol Mol Biol Rev 80:745–763. https://doi.org/10.1128/MMBR.00011-16.
31. Moller AG, Lindsay JA, Read TD. 2019. Determinants of phage host range in *Staphylococcus* species. Appl Environ Microbiol 85:e00209-19. https://doi.org/10.1128/AEM.00209-19.
32. Mo CY, Mathai J, Rostol JT, Varble A, Banh DV, Marraffini LA. 2021. Type III-A CRISPR immunity promotes mutagenesis of staphylococci. Nature 592:611–615. https://doi.org/10.1038/s41586-021-03440-3.
33. Winstel V, Liang C, Sanchez-Carballo P, Steglich M, Munar M, Broker BM, Penadés JR, Nubel U, Holst O, Dandekar T, Peschel A, Xia G. 2013. Wall teichoic acid structure governs horizontal gene transfer between major bacterial pathogens. Nat Commun 4:2345. https://doi.org/10.1038/ncomms3345.
34. Nordström K, Forsgren A. 1974. Effect of protein A on adsorption of bacteriophages to *Staphylococcus aureus*. J Virol 14:198–202. https://doi.org/10.1128/JVI.14.2.198-202.1974.
35. Moller AG, Winston K, Ji S, Wang J, Hargita Davis MN, Solis-Lemus CR, Read TD. 2021. Genes influencing phage host range in *Staphylococcus aureus* on a species-wide scale. mSphere 6:e01263-20. https://doi.org/10.1128/mSphere.01263-20.
36. Ibarra-Chávez R, Brady A, Chen J, Penadés JR, Haag AF. 2022. Phage-inducible chromosomal islands promote genetic variability by blocking phage reproduction and protecting transductants from phage lysis. PLoS Genet 18:e1010146. https://doi.org/10.1371/journal.pgen.1010146.
37. Stone E, Campbell K, Grant I, McAuliffe O. 2019. Understanding and exploiting phage-host interactions. Viruses 11:567. https://doi.org/10.3390/v11060567.
38. Pantůcek R, Rosypalová A, Doskar J, Kailerová J, Růzicková V, Borecká P, Snopková S, Horváth R, Götz F, Rosypal S. 1998. The polyvalent staphylococcal phage $\varphi$812: its host-range mutants and related phages. Virology 246:241–252. https://doi.org/10.1006/viro.1998.9203.
39. Kwan T, Liu J, DuBow M, Gros P, Pelletier J. 2005. The complete genomes and proteomes of 27 *Staphylococcus aureus* bacteriophages. Proc Natl Acad Sci U S A 102:5174–5179. https://doi.org/10.1073/pnas.0501140102.
40. Lepuschitz S, Huhulescu S, Hyden P, Springer B, Rattei T, Allerberger F, Mach RL, Ruppitsch W. 2018. Characterization of a community-acquired-MRSA USA300 isolate from a river sample in Austria and whole genome sequence based comparison to a diverse collection of USA300 isolates. Sci Rep 8:9467. https://doi.org/10.1038/s41598-018-27781-8.
41. Charpentier E, Anton AI, Barry P, Alfonso B, Fang Y, Novick RP. 2004. Novel cassette-based shuttle vector system for Gram-positive bacteria. Appl Environ Microbiol 70:6076–6085. https://doi.org/10.1128/AEM.70.10.6076-6085.2004.
42. Kahánková J, Pantůček R, Goerke C, Růžičková V, Holochová P, Doškař J. 2010. Multilocus PCR typing strategy for differentiation of *Staphylococcus aureus* siphoviruses reflecting their modular genome structure. Environ Microbiol 12:2527–2538. https://doi.org/10.1111/j.1462-2920.2010.02226.x.
43. Coombs GW, Baines SL, Howden BP, Swenson KM, O'Brien FG. 2020. Diversity of bacteriophages encoding Panton-Valentine leukocidin in temporally and geographically related *Staphylococcus aureus*. PLoS One 15:e0228676. https://doi.org/10.1371/journal.pone.0228676.
44. Goerke C, Pantucek R, Holtfreter S, Schulte B, Zink M, Grumann D, Bröker BM, Doskar J, Wolz C. 2009. Diversity of prophages in dominant *Staphylococcus aureus* clonal lineages. J Bacteriol 191:3462–3468. https://doi.org/10.1128/JB.01804-08.
45. Göller PC, Elsener T, Lorgé D, Radulovic N, Bernardi V, Naumann A, Amri N, Khatchatourova E, Coutinho FH, Loessner MJ, Gómez-Sanz E. 2021. Multi-species host range of staphylococcal phages isolated from wastewater. Nat Commun 12:6965. https://doi.org/10.1038/s41467-021-27037-6.
46. Gobl C, Kosol S, Stockner T, Ruckert HM, Zangger K. 2010. Solution structure and membrane binding of the toxin *fst* of the par addiction module. Biochemistry 49:6567–6575. https://doi.org/10.1021/bi1005128.
47. Weaver KE, Weaver DM, Wells CL, Waters CM, Gardner ME, Ehli EA. 2003. *Enterococcus faecalis* plasmid pAD1-encoded Fst toxin affects membrane permeability and alters cellular responses to lantibiotics. J Bacteriol 185:2169–2177. https://doi.org/10.1128/JB.185.7.2169-2177.2003.
48. Sayed N, Nonin-Lecomte S, Rety S, Felden B. 2012. Functional and structural insights of a *Staphylococcus aureus* apoptotic-like membrane peptide from a toxin-antitoxin module. J Biol Chem 287:43454–43463. https://doi.org/10.1074/jbc.M112.402693.
49. Arcus V. 2002. OB-fold domains: a snapshot of the evolution of sequence, structure and function. Curr Opin Struct Biol 12:794–801. https://doi.org/10.1016/S0959-440X(02)00392-5.
50. Domingues S, McGovern S, Plochocka D, Santos MA, Ehrlich SD, Polard P, Chopin MC. 2008. The lactococcal abortive infection protein AbiP is membrane-anchored and binds nucleic acids. Virology 373:14–24. https://doi.org/10.1016/j.virol.2007.11.004.
51. Guo L, Sattler L, Shafqat S, Graumann PL, Bramkamp M. 2022. A bacterial dynamin-like protein confers a novel phage resistance strategy on the population level in *Bacillus subtilis*. mBio 13:e03753-21. https://doi.org/10.1128/mbio.03753-21.
52. Lau RK, Ye Q, Birkholz EA, Berg KR, Patel L, Mathews IT, Watrous JD, Ego K, Whiteley AT, Lowey B, Mekalanos JJ, Kranzusch PJ, Jain M, Pogliano J, Corbett KD. 2020. Structure and mechanism of a cyclic trinucleotide-activated bacterial endonuclease mediating bacteriophage immunity. Mol Cell 77:723–733. https://doi.org/10.1016/j.molcel.2019.12.010.
53. Lopatina A, Tal N, Sorek R. 2020. Abortive infection: bacterial suicide as an antiviral immune strategy. Annu Rev Virol 7:371–384. https://doi.org/10.1146/annurev-virology-011620-040628.
54. Belley A, Callejo M, Arhin F, Dehbi M, Fadhil I, Liu J, McKay G, Srikumar R, Bauda P, Bergeron D, Ha N, Dubow M, Gros P, Pelletier J, Moeck G. 2006. Competition of bacteriophage polypeptides with native replicase proteins for binding to the DNA sliding clamp reveals a novel mechanism for DNA replication arrest in *Staphylococcus aureus*. Mol Microbiol 62:1132–1143. https://doi.org/10.1111/j.1365-2958.2006.05427.x.
55. Rees PJ, Fry BA. 1981. The replication of bacteriophage K DNA in *Staphylococcus aureus*. J Gen Virol 55:41–51. https://doi.org/10.1099/0022-1317-55-1-41.
56. Parma DH, Snyder M, Sobolevski S, Nawroz M, Brody E, Gold L. 1992. The Rex system of bacteriophage lambda: tolerance and altruistic cell death. Genes Dev 6:497–510. https://doi.org/10.1101/gad.6.3.497.
57. Tremblay C, Bédard M, Bonin MA, Lavigne P. 2016. Solution structure of the 13th C2H2 zinc finger of Miz-1. Biochem Biophys Res Commun 473:471–475. https://doi.org/10.1016/j.bbrc.2016.03.034.
58. Li Y, Haarhuis JHI, Sedeno Cacciatore A, Oldenkamp R, van Ruiten MS, Willems L, Teunissen H, Muir KW, de Wit E, Rowland BD, Panne D. 2020.

Downloaded from https://journals.asm.org/journal/mbio on 08 August 2023 by 144.32.224.27.

The structural basis for cohesin-CTCF-anchored loops. Nature 578:472–476. https://doi.org/10.1038/s41586-019-1910-z.
59. Shah M, Taylor VL, Bona D, Tsao Y, Stanley SY, Pimentel-Elardo SM, McCallum M, Bondy-Denomy J, Howell PL, Nodwell JR, Davidson AR, Moraes TF, Maxwell KL. 2021. A phage-encoded anti-activator inhibits quorum sensing in *Pseudomonas aeruginosa*. Mol Cell 81:571–583. https://doi.org/10.1016/j.molcel.2020.12.011.
60. Owen SV, Wenner N, Dulberger CL, Rodwell EV, Bowers-Barnard A, Quinones-Olvera N, Rigden DJ, Rubin EJ, Garner EC, Baym M, Hinton JCD. 2021. Prophages encode phage-defense systems with cognate self-immunity. Cell Host Microbe 29:1620–1633. https://doi.org/10.1016/j.chom.2021.09.002.
61. Xia G, Corrigan RM, Winstel V, Goerke C, Grundling A, Peschel A. 2011. Wall teichoic acid-dependent adsorption of staphylococcal siphovirus and myovirus. J Bacteriol 193:4006–4009. https://doi.org/10.1128/JB.01412-10.
62. Doškar J, Pallová P, Pantucek R, Rosypal S, Ruzicková V, Pantucková P, Kailerová J, Klepárník K, Malá Z, Bocek P. 2000. Genomic relatedness of *Staphylococcus aureus* phages of the International Typing Set and detection of serogroup A, B, and F prophages in lysogenic strains. Can J Microbiol 46:1066–1076. https://doi.org/10.1139/cjm-46-11-1066.
63. Novick RP. 1963. Analysis by transduction of mutations affecting penicillinase formation in *Staphylococcus aureus*. J Gen Microbiol 33:121–136. https://doi.org/10.1099/00221287-33-1-121.
64. Borecká P, Rosypal S, Pantůcek R, Doskar J. 1996. Localization of prophages of serological group B and F on restriction fragments defined in the restriction map of *Staphylococcus aureus* NCTC 8325. FEMS Microbiol Lett 143:203–210. https://doi.org/10.1111/j.1574-6968.1996.tb08481.x.
65. Pantůcek R, Doskar J, Růzicková V, Kaspárek P, Orácová E, Kvardová V, Rosypal S. 2004. Identification of bacteriophage types and their carriage in *Staphylococcus aureus*. Arch Virol 149:1689–1703. https://doi.org/10.1007/s00705-004-0335-6.
66. Bae T, Baba T, Hiramatsu K, Schneewind O. 2006. Prophages of *Staphylococcus aureus* Newman and their contribution to virulence. Mol Microbiol 62:1035–1047. https://doi.org/10.1111/j.1365-2958.2006.05441.x.
67. Augustin J, Götz F. 1990. Transformation of *Staphylococcus epidermidis* and other staphylococcal species with plasmid DNA by electroporation. FEMS Microbiol Lett 66:203–207. https://doi.org/10.1111/j.1574-6968.1990.tb03997.x.
68. Mašlaňová I, Doškař J, Varga M, Kuntová L, Mužík J, Malúšková D, Růžičková V, Pantůcek R. 2013. Bacteriophages of *Staphylococcus aureus* efficiently package various bacterial genes and mobile genetic elements including SCC*mec* with different frequencies. Environ Microbiol Rep 5:66–73. https://doi.org/10.1111/j.1758-2229.2012.00378.x.
69. Zeman M, Mašlaňová I, Indráková A, Šiborová M, Mikulášek K, Bendíčková K, Plevka P, Vrbovská V, Zdráhal Z, Doškař J, Pantůcek R. 2017. *Staphylococcus sciuri* bacteriophages double-convert for staphylokinase and phospholipase, mediate interspecies plasmid transduction, and package mecA gene. Sci Rep 7:46319. https://doi.org/10.1038/srep46319.
70. Zheng X, Marsman G, Lacey KA, Chapman JR, Goosmann C, Ueberheide BM, Torres VJ. 2021. The cell envelope of *Staphylococcus aureus* selectively controls the sorting of virulence factors. Nat Commun 12:6193. https://doi.org/10.1038/s41467-021-26517-z.
71. Novo DJ, Perlmutter NG, Hunt RH, Shapiro HM. 2000. Multiparameter flow cytometric analysis of antibiotic effects on membrane potential, membrane permeability, and bacterial counts of *Staphylococcus aureus* and *Micrococcus luteus*. Antimicrob Agents Chemother 44:827–834. https://doi.org/10.1128/AAC.44.4.827-834.2000.
72. Krogh A, Larsson B, von Heijne G, Sonnhammer EL. 2001. Predicting transmembrane protein topology with a hidden Markov model: application to complete genomes. J Mol Biol 305:567–580. https://doi.org/10.1006/jmbi.2000.4315.
73. Yan J, Kurgan L. 2017. DRNApred, fast sequence-based method that accurately predicts and discriminates DNA- and RNA-binding residues. Nucleic Acids Res 45:e84. https://doi.org/10.1093/nar/gkx059.
74. Soding J, Biegert A, Lupas AN. 2005. The HHpred interactive server for protein homology detection and structure prediction. Nucleic Acids Res 33:W244–W248. https://doi.org/10.1093/nar/gki408.
75. Kelley LA, Mezulis S, Yates CM, Wass MN, Sternberg MJ. 2015. The Phyre2 web portal for protein modeling, prediction and analysis. Nat Protoc 10:845–858. https://doi.org/10.1038/nprot.2015.053.
76. Holm L, Rosenstrom P. 2010. Dali server: conservation mapping in 3D. Nucleic Acids Res 38:W545–W549. https://doi.org/10.1093/nar/gkq366.
77. Jumper J, Evans R, Pritzel A, Green T, Figurnov M, Ronneberger O, Tunyasuvunakool K, Bates R, Zidek A, Potapenko A, Bridgland A, Meyer C, Kohl SAA, Ballard AJ, Cowie A, Romera-Paredes B, Nikolov S, Jain R, Adler J, Back T, Petersen S, Reiman D, Clancy E, Zielinski M, Steinegger M, Pacholska M, Berghammer T, Bodenstein S, Silver D, Vinyals O, Senior AW, Kavukcuoglu K, Kohli P, Hassabis D. 2021. Highly accurate protein structure prediction with AlphaFold. Nature 596:583–589. https://doi.org/10.1038/s41586-021-03819-2.
78. Pettersen EF, Goddard TD, Huang CC, Couch GS, Greenblatt DM, Meng EC, Ferrin TE. 2004. UCSF Chimera - a visualization system for exploratory research and analysis. J Comput Chem 25:1605–1612. https://doi.org/10.1002/jcc.20084.
79. Pettersen EF, Goddard TD, Huang CC, Meng EC, Couch GS, Croll TI, Morris JH, Ferrin TE. 2021. UCSF ChimeraX: structure visualization for researchers, educators, and developers. Protein Sci 30:70–82. https://doi.org/10.1002/pro.3943.
80. Fišarová L, Botka T, Du X, Mašlaňová I, Bárdy P, Pantůček R, Benešík M, Roudnický P, Winstel V, Larsen J, Rosenstein R, Peschel A, Doškař J. 2021. *Staphylococcus epidermidis* phages transduce antimicrobial resistance plasmids and mobilize chromosomal islands. mSphere 6:e00223-21. https://doi.org/10.1128/mSphere.00223-21.
81. Bolger AM, Lohse M, Usadel B. 2014. Trimmomatic: a flexible trimmer for Illumina sequence data. Bioinformatics 30:2114–2120. https://doi.org/10.1093/bioinformatics/btu170.
82. Wick RR, Judd LM, Gorrie CL, Holt KE. 2017. Unicycler: resolving bacterial genome assemblies from short and long sequencing reads. PLoS Comput Biol 13:e1005595. https://doi.org/10.1371/journal.pcbi.1005595.
83. Walker BJ, Abeel T, Shea T, Priest M, Abouelliel A, Sakthikumar S, Cuomo CA, Zeng Q, Wortman J, Young SK, Earl AM. 2014. Pilon: an integrated tool for comprehensive microbial variant detection and genome assembly improvement. PLoS One 9:e112963. https://doi.org/10.1371/journal.pone.0112963.
84. Li W, O'Neill KR, Haft DH, DiCuccio M, Chetvernin V, Badretdin A, Coulouris G, Chitsaz F, Derbyshire MK, Durkin AS, Gonzales NR, Gwadz M, Lanczycki CJ, Song JS, Thanki N, Wang J, Yamashita RA, Yang M, Zheng C, Marchler-Bauer A, Thibaud-Nissen F. 2021. RefSeq: expanding the Prokaryotic Genome Annotation Pipeline reach with protein family model curation. Nucleic Acids Res 49:D1020–D1028. https://doi.org/10.1093/nar/gkaa1105.
85. Jolley KA, Bray JE, Maiden MCJ. 2018. Open-access bacterial population genomics: BIGSdb software, the PubMLST.org website and their applications. Wellcome Open Res 3:124. https://doi.org/10.12688/wellcomeopenres.14826.1.
86. Harmsen D, Claus H, Witte W, Rothganger J, Claus H, Turnwald D, Vogel U. 2003. Typing of methicillin-resistant *Staphylococcus aureus* in a university hospital setting by using novel software for spa repeat determination and database management. J Clin Microbiol 41:5442–5448. https://doi.org/10.1128/JCM.41.12.5442-5448.2003.
87. Bikandi J, San Millan R, Rementeria A, Garaizar J. 2004. *In silico* analysis of complete bacterial genomes: PCR, AFLP-PCR and endonuclease restriction. Bioinformatics 20:798–799. https://doi.org/10.1093/bioinformatics/btg491.
88. Solovyev V, Salamov A. 2011. Automatic annotation of microbial genomes and metagenomic sequences, p 61–78. *In* Li RW (ed), Metagenomics and its applications in agriculture, biomedicine and environmental studies, vol 1. Nova Science Publishers, Hauppauge, NY.
89. Macke TJ, Ecker DJ, Gutell RR, Gautheret D, Case DA, Sampath R. 2001. RNAMotif, an RNA secondary structure definition and search algorithm. Nucleic Acids Res 29:4724–4735. https://doi.org/10.1093/nar/29.22.4724.
90. Meier-Kolthoff JP, Goker M. 2017. VICTOR: genome-based phylogeny and classification of prokaryotic viruses. Bioinformatics 33:3396–3404. https://doi.org/10.1093/bioinformatics/btx440.
91. Lefort V, Desper R, Gascuel O. 2015. FastME 2.0: a comprehensive, accurate, and fast distance-based phylogeny inference program. Mol Biol Evol 32:2798–2800. https://doi.org/10.1093/molbev/msv150.
92. Kaneko J, Kimura T, Narita S, Tomita T, Kamio Y. 1998. Complete nucleotide sequence and molecular characterization of the temperate staphylococcal bacteriophage φPVL carrying Panton–Valentine leukocidin genes. Gene 215:57–67. https://doi.org/10.1016/S0378-1119(98)00278-9.
93. Kittl S, Brodard I, Overesch G, Kuhnert P, Jores J, Labroussaa F. 2021. Complete genome sequences of the methicillin-resistant strain *Staphylococcus aureus* 17Gst354 and its prophage *Staphylococcus* phage vB_StaphS-IVBph354. Microbiol Resour Announc 10:e0058621. https://doi.org/10.1128/MRA.00586-21.
94. Paredes C, Chi SI, Flint A, Weedmark K, McDonald C, Bearne J, Ramirez-Arcos S, Pagotto F. 2021. Complete genome sequence of *Staphylococcus aureus* PS/BAC/169/17/W, isolated from a contaminated platelet concentrate in England. Microbiol Resour Announc 10:e00841-21. https://doi.org/10.1128/MRA.00841-21.



Downloaded from https://journals.asm.org/journal/mbio on 08 August 2023 by 144.32.224.27.

95. Kreiswirth BN, Lofdahl S, Betley MJ, O'Reilly M, Schlievert PM, Bergdoll MS, Novick RP. 1983. The toxic shock syndrome exotoxin structural gene is not detectably transmitted by a prophage. Nature 305:709–712. https://doi.org/10.1038/305709a0.
96. Novick RP. 1967. Properties of a cryptic high-frequency transducing phage in *Staphylococcus aureus*. Virology 33:155–166. https://doi.org/10.1016/0042-6822(67)90105-5.
97. Yoshizawa Y. 1985. Isolation and characterization of restriction negative mutants of *Staphylococcus aureus*. Jikeikai Med J 32:415–421.
98. Diep BA, Gill SR, Chang RF, Phan TH, Chen JH, Davidson MG, Lin F, Lin J, Carleton HA, Mongodin EF, Sensabaugh GF, Perdreau-Remington F. 2006. Complete genome sequence of USA300, an epidemic clone of community-acquired meticillin-resistant *Staphylococcus aureus*. Lancet 367:731–739. https://doi.org/10.1016/S0140-6736(06)68231-7.
99. Rohmer C, Dobritz R, Tuncbilek-Dere D, Lehmann E, Gerlach D, George SE, Bae T, Nieselt K, Wolz C. 2022. Influence of *Staphylococcus aureus* strain background on Sa3int phage life cycle switches. Viruses 14:2471. https://doi.org/10.3390/v14112471.
100. Kuntová L, Pantůček R, Rájová J, Růžičková V, Petráš P, Mašlaňová I, Doškař J. 2012. Characteristics and distribution of plasmids in a clonally diverse set of methicillin-resistant *Staphylococcus aureus* strains. Arch Microbiol 194:607–614. https://doi.org/10.1007/s00203-012-0797-y.
101. Augustin J, Rosenstein R, Wieland B, Schneider U, Schnell N, Engelke G, Entian KD, Gotz F. 1992. Genetic analysis of epidermin biosynthetic genes and epidermin-negative mutants of *Staphylococcus epidermidis*. Eur J Biochem 204:1149–1154. https://doi.org/10.1111/j.1432-1033.1992.tb16740.x.

Downloaded from https://journals.asm.org/journal/mbio on 08 August 2023 by 144.32.224.27.